ChemComm

COMMUNICATION

View Article Online
View Journal | View Issue

Check for updates

Cite this: *Chem. Commun.*, 2024, **60**, 13963

Received 8th August 2024,
Accepted 31st October 2024

DOI: 10.1039/d4cc04037f

rsc.li/chemcomm

Synthesis of environmentally friendly energetic cocrystal derived from commodity chemicals†

Kazuki Inoue,[a] Yosuke Nishiwaki,[b] Mieko Kumasaki, *[c] Shinya Matsumoto[c] and Ken Okada[d]

Ammonium nitrate (AN) is a green oxidizer in the field of energetic materials. However, hygroscopicity and phase transitions have prevented AN from being put into practical use. To address these two drawbacks, a cocrystallization technique was applied to AN in this study. An AN/glycine (Gly) cocrystal was newly prepared and characterized; both AN/Gly and AN/sarcosine exhibited decreased hygroscopicity and did not exhibit a phase transition.

Energetic materials are characterized by their rapid burning and the release of large quantities of heat and gas. They are used in blasting, as propellants, and for military use.[1] Ammonium nitrate (NH_4NO_3; AN) has long been investigated for its application as an oxidizer;[2] oxidizers enhance the activity of combustible materials, facilitating burning and concomitant release of energy. The lack of metallic elements in the chemical formula enables AN to be converted into gas without leaving metal residues behind that can impact the environment, rendering it a promising green oxidizer;[3] conventional oxidizers contain metal species such as K, Sr, and Cu.[4] However, the application of AN is limited by two drawbacks: hygroscopicity and phase transitions.[5] AN is highly hygroscopic, and water absorption significantly affects the burning behaviour of energetic materials using AN.[5a] Moreover, the phase transition of AN is known to lead to volume changes, which complicate its storage.[5b] To address hygroscopicity of AN, various coating agents and methods, such as surfactants, oil, encapsulation, and wax, have been developed.[6] To prevent phase transitions, phase-stabilized AN (PSAN) has been developed and used in practical airbag systems.[7] However, PSAN deteriorates due to its high hygroscopicity, resulting in accidental and unintentionally fast burning.[8]

As a solution to the drawbacks associated with AN, we aimed to apply cocrystallization. Cocrystals are molecular crystals containing two or more neutral molecules, and their enhanced intermolecular interactions lead to decreased hygroscopicity relative to the parent materials, as demonstrated in the field of pharmacy.[9] In addition, cocrystallized materials exhibit different crystal structures from the original materials. As a result, phase transitions associated with the parent materials do not occur in the cocrystallized materials.[10] Therefore, cocrystallization can address both hygroscopicity and phase transition, whereas traditional strategies, such as coating and phase stabilization by adding organic or salt materials, address only one of the two problems. Rodrigues *et al.* reported the synthesis and crystal structure of AN/sarcosine (Sar) cocrystals; however, their physicochemical properties were not characterized.[11] In the crystal structure of the AN/Sar cocrystal, the carboxylic acid and amine functional groups of Sar interact with the ammonium cation and nitrate anion of AN, respectively. Therefore, the structure of the AN/Sar cocrystal implies that the amino acid is a potential cocrystal-former (co-former) of AN. The oxygen balance (OB) of AN/Sar cocrystal is negative, far from zero, which indicates a poor OB (AN/Sar = −61%). The closer the OB of a substance is to zero, the better it is as an energetic material. An OB of zero represents optimal balance for an energetic material because the fuel material and oxidizer can react completely and generate maximum energy. Because Sar itself has a highly negative OB value (−135%), it is not the best component for energetic materials, as it would be difficult to achieve zero OB for the mixture of Sar and any oxidizer. Therefore, we aimed to synthesize a novel AN cocrystal using another amino acid. From the viewpoint of OB, we selected glycine (Gly, OB = −95.9%), which contains relatively few

---

[a] *Graduate School of Environment and Information Sciences, Yokohama National University, 79-7 Tokiwadai, Hodogaya-ku, Yokohama, Kanagawa, 240-8501, Japan*
[b] *National Institute of Occupational Safety and Health, Japan, 1-4-6 Umezono, Kiyose, Tokyo, 204-0024, Japan*
[c] *Faculty of Environment and Information Sciences, Yokohama National University, 79-7 Tokiwadai, Hodogaya-ku, Yokohama, Kanagawa, 240-8501, Japan. E-mail: kumasaki@ynu.ac.jp*
[d] *Research Institute of Science for Safety and Sustainability, National Institute of Advanced Industrial Science and Technology (AIST), AIST Tsukuba Central 5, 1-1-1 Higashi, Tsukuba, Ibaraki, 305-8565, Japan*

† Electronic supplementary information (ESI) available: Experimental section, atomic distances, and results of FT-IR and powder X-ray diffraction. CCDC 2257499. For ESI and crystallographic data in CIF or other electronic format see DOI: **https://doi.org/10.1039/d4cc04037f**

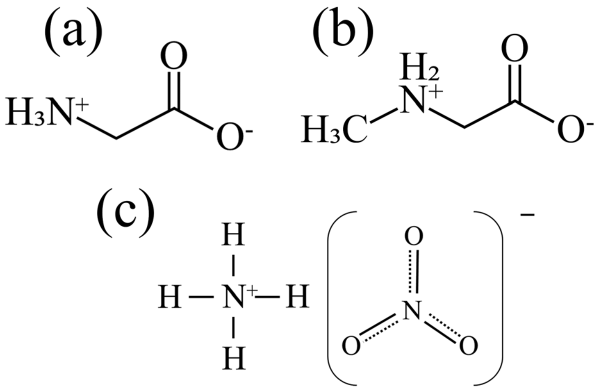

Fig. 1 Molecular structures of: (a) glycine; (b) sarcosine; and (c) ammonium nitrate.

carbon and hydrogen atoms in its molecular formula, as a promising co-former (Fig. 1). In this study, a novel AN/Gly cocrystal was synthesized, and its crystal structure was determined. Furthermore, the physicochemical properties of the AN/Sar and AN/Gly cocrystals were characterized to clarify the effects of cocrystallization on the drawbacks of AN.

Single crystals of AN/Gly were prepared using a cooling method; AN and Gly (2 : 1) were dissolved in deionized water at room temperature and the solution was then cooled at 4 °C. Plate-like crystals precipitated from the solution over the course of three days.

The crystal structure of AN/Gly is shown in Fig. 2. The AN/Gly cocrystal is monoclinic (a = 5.7762(1) Å, b = 22.1425(4) Å, c = 7.9135(1) Å, β = 92.015(2)°, Z = 4) and crystallizes in the $P2_1/c$ space group (Table S1, Cambridge Structural Database deposition number: 2257499, ESI†). AN and Gly are present in the cocrystal in a 2 : 1 ratio, whereas the ratio of AN/Sar is 1 : 1. Each column of Gly is surrounded by six columns of AN, and the hydrogen bond between O2···H1C–N1 connects the Gly molecules. Ammonium ions form hydrogen bonds with the two O-atoms of Gly, and the nitrate ions interact with the N–H bonds of Gly (Table S2, ESI†). Two ammonium ions in AN/Gly form stronger hydrogen bonds than those in pristine AN. The shortest hydrogen bond distances formed by the ammonium ion of AN are 2.935 Å (D···A), while the ones in AN/Gly are 2.838 (2) and 2.833 (1) Å.[12] These results indicate that the ammonium ions were stabilized by cocrystallization compared with pristine AN. The OB for AN/Gly is −17%, which is better than that of AN/Sar (−61%) because of the higher content of oxidizer. In addition, the calculated density of AN/Gly is 1.544 g cm^{-3}.

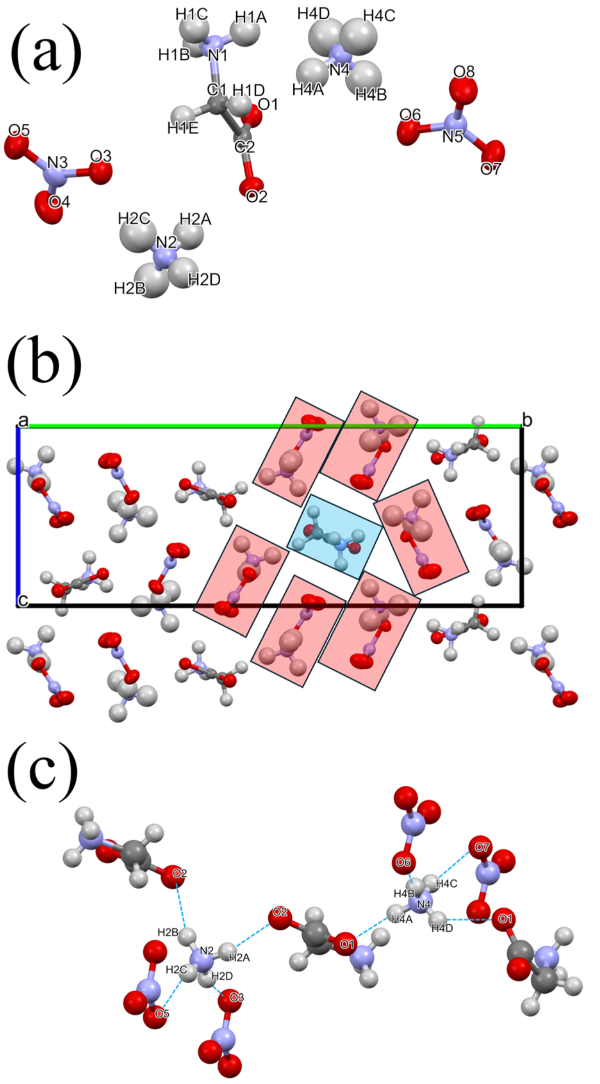

Fig. 2 Crystal structure for AN/Gly: (a) asymmetric unit of AN/Gly; the thermal ellipsoids are depicted at the 50% probability level; (b) crystal packing viewed from the a axis. A Gly column and six AN columns are highlighted in blue and red, respectively; (c) hydrogen bonds around ammonium ions. Hydrogen bonds are displayed in the blue lines.

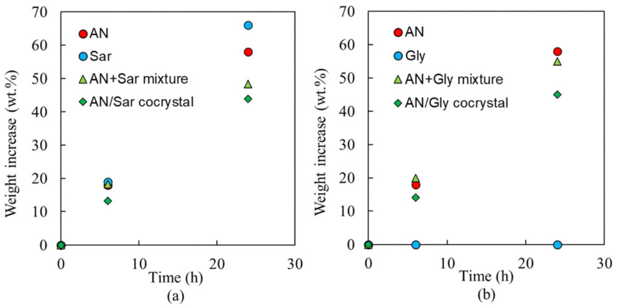

Fig. 3 Results from the hygroscopicity tests for: (a) Sar-containing samples and (b) Gly-containing samples.

Samples (0.5 g) were stored in a sealed container at a controlled temperature (30 °C) and relative humidity (RH; saturated salt method with NaCl, RH = 75%) using a thermostat.[13] The samples of cocrystals were prepared by liquid-assisted grinding (LAG) using water as an additive because the LAG method enables quick preparation of large amounts of samples. The sample masses were measured after 6 and 24 h; the results are shown in Fig. 3. The physical mixtures of each parent material were used as reference. Sar showed higher hygroscopicity than AN, whereas Gly did not absorb moisture. The mixtures of each parent material showed absorptions of 48% and 55% for AN + Sar and AN + Gly after 24 h,

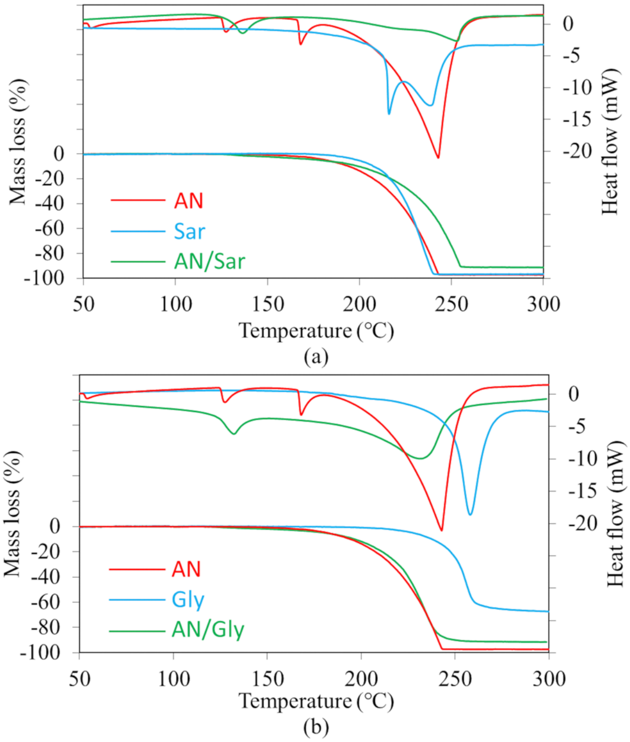

Fig. 4 TG-DTA results for: (a) AN, Sar, and AN/Sar; and (b) AN, Gly, and AN/Gly.

respectively. Both cocrystals exhibited lower hygroscopicity relative to crude mixtures of the cocrystal components and pristine AN. Moreover, a 45% weight increase was observed for AN/Gly after 24 h, which is much lower than that of AN + Gly. As shown by X-ray crystallography, the ammonium ions of AN/Gly form stronger hydrogen bonds than those in pristine AN. Strengthened hydrogen bonds *via* cocrystallization hinder the penetration of water into the crystal and the formation of hydrogen bonds between ammonium ions and water molecules in the air, leading to decreased hygroscopicity.[14]

Thermogravimetry-differential thermal analysis (TG-DTA) was conducted to investigate the thermal behaviour of the cocrystals (Fig. 4). The cocrystal samples prepared by the cooling method were used for thermal analyses. While pristine AN showed phase transitions at 53 and 128 °C, neither cocrystal showed a phase transition. Similar to the case of mixed crystals of AN, the introduction of Gly in AN resulted in different hydrogen bonds between Gly and AN, accompanying different crystal packing from pristine AN, suppressing the phase transition.[15] The onset temperatures of the endothermic peaks from melting occurred at 128 °C for AN/Sar and 123 °C for AN/Gly, which were lower than those of pristine AN. The average mass loss during AN/Gly decomposition was 85%.

Differential scanning calorimetry (DSC) also revealed that no phase transition occurred in the two cocrystals (Fig. 5). The decomposition temperature (T_{onset}) of AN/Gly (234 °C) was lower than that of AN (267 °C) and AN/Sar (263 °C). The calorific value of decomposition peak of AN/Gly was 3.16 kJ g^{-1}, which was much higher than those of AN (1.68 kJ g^{-1}) and AN/Sar (1.53 kJ g^{-1}) because of its enhanced OB. In fact, it is higher than that of 3-nitro-1,2,4-triazol-5-one (2.97 kJ g^{-1}), which is commonly used as a component of insensitive energetic materials.[16]

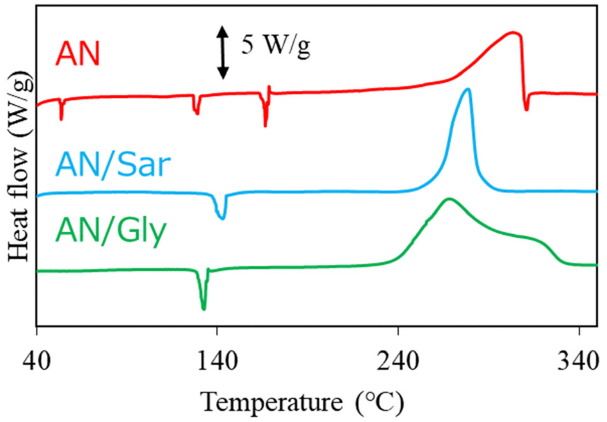

Fig. 5 DSC results for AN, AN/Sar, and AN/Gly.

To investigate phase stabilization further, cyclic DSC analysis was conducted on the AN/Gly cocrystal (Fig. 6). No phase transition was observed in the heating and cooling regimes. Therefore, cocrystallization has accomplished phase stabilization of AN.

Energetic materials explode inadvertently in response to stimuli such as friction and impact. Therefore, evaluating their sensitivity is important for safety. Friction sensitivity tests were conducted using a BAM friction sensitivity tester. Six trials deploying a 353.0 N load were conducted. None of the cocrystals exploded during the six trials, indicating they are sufficiently safe for handling.

An environmentally friendly energetic cocrystal, AN/Gly, was synthesized using commodity chemicals of low-toxicity. Humidity tests showed that the hygroscopicity of AN was suppressed by cocrystallization. Furthermore, thermal analysis revealed that phase transitions associated with AN were not observed in either AN/Sar or AN/Gly. The disappearance of this phase transition alludes to the potential application of AN in various devices. Furthermore, the calorific value of AN/Gly was much higher than that of AN. These results suggest that cocrystallization is effective for addressing both the hygroscopicity and phase transition of AN. Therefore, cocrystallization of AN with commodity chemicals is a promising method for obtaining green, energetic materials with improved properties relative to the parent components.

Kazuki Inoue conducted synthesis, X-ray studies, FT-IR, thermal and elemental analysis, and sensitivity test and wrote a paper; Yosuke Nishiwaki performed synthesis, thermal analysis, and humidity test; Shinya Matsumoto contribute to crystallographic study; Ken Okada contribute to sensitivity test; Mieko Kumasaki managed the project.

The authors are grateful to the Instrumental Analysis Center of Yokohama National University for providing access to the single-crystal X-ray diffraction, powder X-ray diffraction, elemental analysis, and Fourier-transform infrared spectroscopy

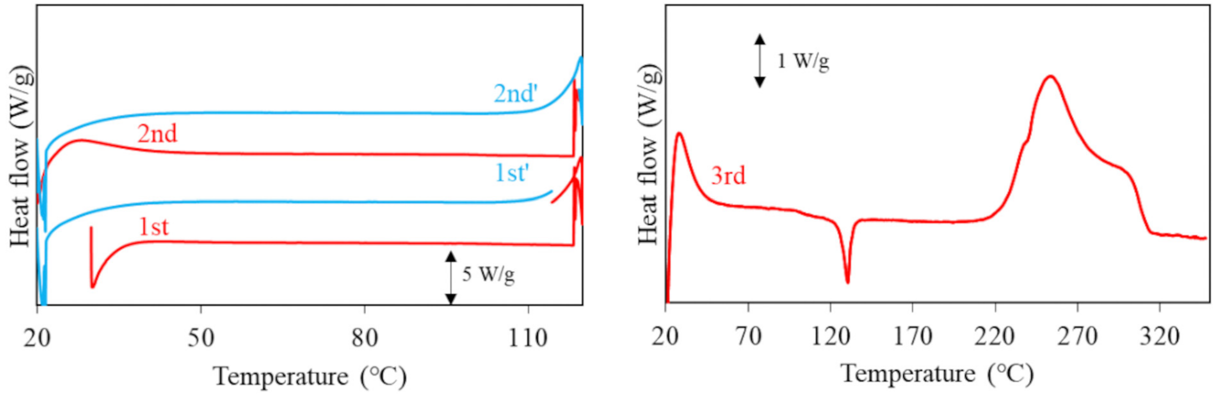

Fig. 6 Results of cyclic DSC for AN/Gly. Red lines show heating processes and blue lines show cooling processes. The left figure shows the first and second heating/cooling cycle and the right figure shows the third heating process.

facilities. This study was financially supported by the Foundation for the Promotion of Industrial Explosives Technology and the Collaborative Investigation Promotion Program Task C of Yokohama National University. In addition, we express our deepest appreciation to the Japan Explosives Industry Association.

Data availability

Crystallographic data for AN/Gly has been deposited at the CCDC under 2257499 and can be obtained from **https://www.ccdc.cam.ac.uk/**. The data supporting this article have been included as part of the ESI.†

Conflicts of interest

There are no conflicts to declare.

Notes and references

1 (*a*) T. M. Klapötke, *Chemistry of high energy materials*, de Gruyter GmbH, Berlin/Boston, 6th edn, 2022, vol. 1, pp. 1–12; (*b*) T. Brink, in *Green Energetic Materials*, ed. T. Brink, John Willey & Sons Ltd., Chichester, 2014, vol. 1, pp. 1–11.

2 (*a*) H. Tsuchiya, R. Togashi and M. Kohga, *Prop., Explos., Pyrotech.*, 2023, **48**, e202300027; (*b*) A. Abdelaziz, D. Trache, A. F. Tarchoun, H. Boukeciat, D. E. Kadri, H. Hassam, S. Ouahioune, N. Sahnoun, S. Thakur and T. M. Klapötke, *Chem. Eng. J.*, 2024, **487**, 150654; (*c*) M. Kohga and R. Togashi, *Propellants, Explos., Pyrotech.*, 2021, **46**, 1016–1022.

3 C. Oommen and S. R. Jain, *J. Hazard. Mater.*, 1999, **67**, 253–281.

4 (*a*) M. Nakashima, T. Itaura, H. Matsunaga, E. Higashi, S. Takagi and K. Katoh, *J. Therm. Anal. Calorim.*, 2018, **131**, 95–100; (*b*) M. Nakashima, H. Matsunaga, E. Higashi, S. Takagi and K. Katoh, *Sci. Technol. Energ. Mater.*, 2019, **80**(5), 183–187; (*c*) K. Hasue and M. Matsukawa, *Sci. Technol. Energ. Mater.*, 2016, **77**(5), 111–116; (*d*) Y. Miyata, K. Baba, S. Date and K. Hasue, *Sci. Technol. Energ. Mater.*, 2004, **65**(5), 167–172; (*e*) K. Hasue and K. Yoshitake, *Sci. Technol. Energ. Mater.*, 2013, **74**(3), 66–72.

5 (*a*) B. I. Elzaki and Y. J. Zhang, *Def. Technol.*, 2019, **15**, 615–620; (*b*) K. Shiota, H. Matsunaga and A. Miyake, *J. Therm. Anal. Calorim.*, 2017, **127**, 851–856.

6 (*a*) F. Ali, B. M. P. Pingua, A. Dey, M. P. Roy and P. K. Singh, *Propellants, Explos., Pyrotech.*, 2021, **46**(1), 78–83; (*b*) R. S. Damse, *Def. Sci. J.*, 2004, **54**(4), 483–492; (*c*) B. I. Elzaki and Y. J. Zhang, *Def. Technol.*, 2019, **15**(4), 615–620; (*d*) A. Asaji, M. Kitajima, T. Yamaguchi, N. Muroya and M. Morishita, *Canada Pat.*, CA925380A, 1970.

7 J. H. Kim, *J. Chem. Eng. Jpn.*, 1997, **30**(2), 336–338.

8 T. R. Ravindran, R. Rajan and V. Venkatesan, *J. Phys. Chem. C*, 2019, **123**, 29067–29085.

9 (*a*) A. V. Trask, W. D. S. Motherwell and W. Jones, *Int. J. Pharm.*, 2006, **320**, 114–123; (*b*) A. V. Trask, W. D. S. Motherwell and W. Jones, *Cryst. Growth Des.*, 2005, **5**(3), 1013–1021; (*c*) Y. P. Nugraha and H. Uekusa, *CrystEngComm*, 2018, **20**, 2653; (*d*) R. D. Davies, N. J. Vigilante, A. D. Frederick, V. S. Mandala and M. A. Mehta, *J. Chem. Crystallogr.*, 2022, **54**, 479–484.

10 (*a*) A. J. Bennett, L. M. Foroughi and A. J. Matzger, *J. Am. Chem. Soc.*, 2024, **146**(3), 1771–1775; (*b*) A. J. Bennett and A. J. Matzger, *Chem. – Eur. J.*, 2023, **29**, e202300076.

11 V. H. Rodrigues, M. R. Silva, A. M. Beja, J. A. Paixão and M. M. R. R. Costa, *Acta Crystallogr., Sect. E: Struct. Rep. Online*, 2005, **61**, o1631–o1633.

12 C. S. Choi, J. E. Mapes and E. Prince, *Acta Crystallogr., Sect. B: Struct. Crystallogr. Cryst. Chem.*, 1972, **28**, 1357–1361.

13 L. Greenspan, *J. Res. Natl. Bur. Stand., Sect. A*, 1977, **81**(1), 89–96.

14 J. Cui, J. Han, J. Wang and R. Huang, *J. Chem. Eng. Data*, 2010, **55**(9), 3229–3234.

15 N. I. Golovina, G. N. Nechiporenko, G. G. Nemtsev, G. P. Dolganova, V. P. Roshchupkin, D. B. Lempert and G. B. Manelis, *Russ. J. Appl. Chem.*, 2007, **80**(1), 24–30.

16 (*a*) Physical Hazard Database of chemicals, **https://explosion-safety.securesite.jp/index_e.htm**, accessed June 2024; (*b*) D. Frem, *Propellants Explos. Pyrotech.*, 2023, **48**, e202100312.